Identification and Visualization of Sound Sources with Non-regular Shapes Using the Inverse Vibro-acoustic Technique

Jeong-Guon Ih

Center for Noise & Vibration Control (NOVIC)
Department of Mechanical Engineering

Korea Advanced Institute of Science & Technology

KAIST

Various Source Identification Techniques

- Selective operation, cocooning & exposure (window) techniques
- Ducted measurement
- Use of directional or focusing microphones
- Surface intensity / Acoustic intensity techniques
- Structural intensity technique
- Signal processing techniques (multiple or partial coherences, sonoplot, etc.)
- Statistical energy analysis (SEA) technique
- Transfer path analysis (or vector analysis combined with PCA) technique
- Optical holography technique (SLDV, DPLDI, ESPI)
- Array microphones (or beam forming) technique, etc.

- ***Acoustic imaging (or holography) technique***

Indirect Methods

- /

Acou
i-Sp
iFRF
NAH-*sp*FT
NAH-iBEM

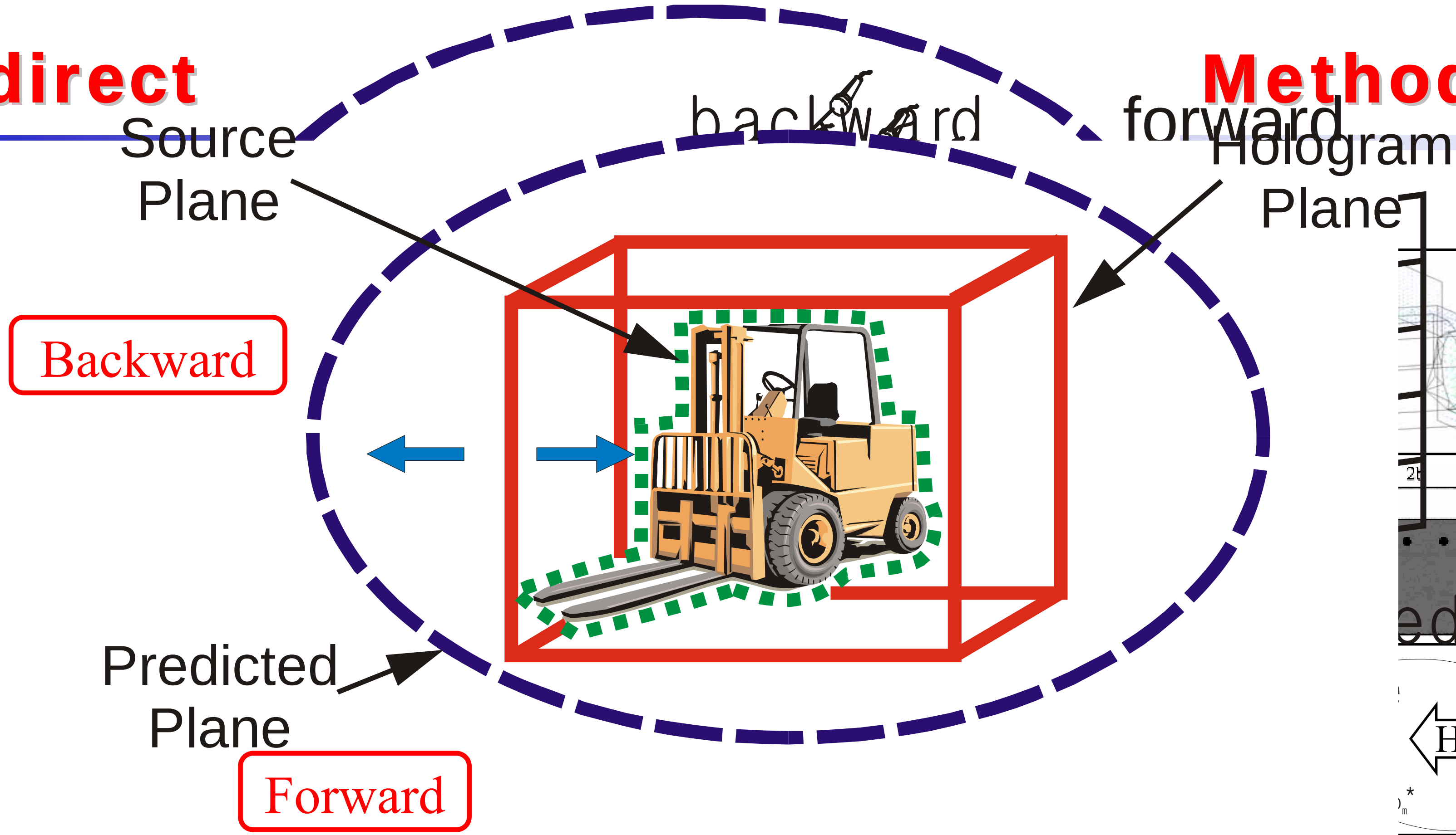

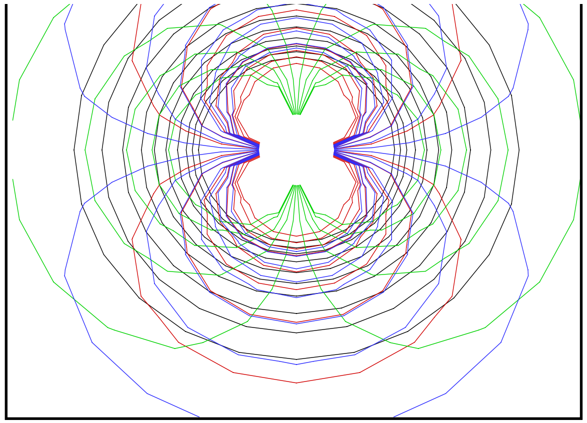

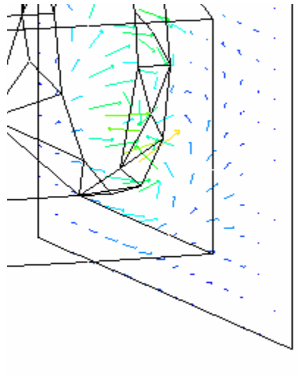

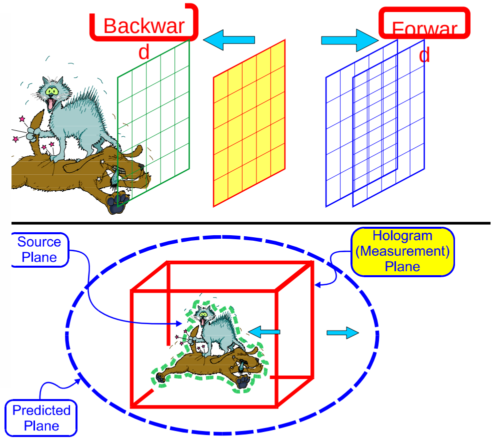

Measuring Distance from Source Surface?

- ***Far & Near Field***
  - Rayleigh distance: $\frac{r}{\lambda} >> \left(\frac{L}{\lambda}\right)^2$ or $r >> \frac{L^2}{\lambda}$
  - Rule of thumb: $R \geq \lambda$ or $R \geq L_{\max}$

- ***Measurement Field***
  - Close near-field measurement: (ex) NAH
  - Far-field measurement: (ex) SPL, Beam forming
  - Intermediate near-field measurement: (ex) AI, HELS, iFRF

- ***Close near-field***
  - Rich content of evanescent wave components
  - Excellent S/N-ratio
  - Small number of sensors (Small size measurement plane)

Distance of Hologram Plane: (4,3) mode at 288 Hz

Steel plate (1t)
500 X 500 mm

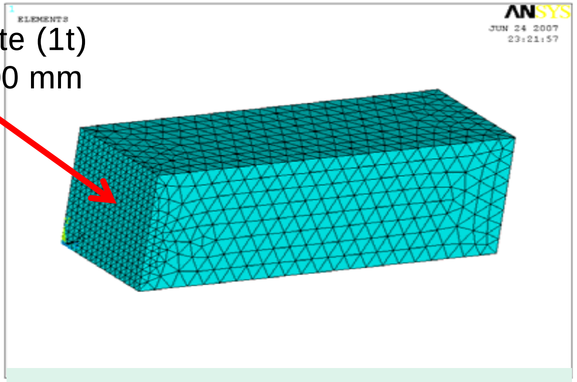

1137 nodes
2270 triangular linear ele'ts
h_{max} = 0.09 m (f < 630 Hz)

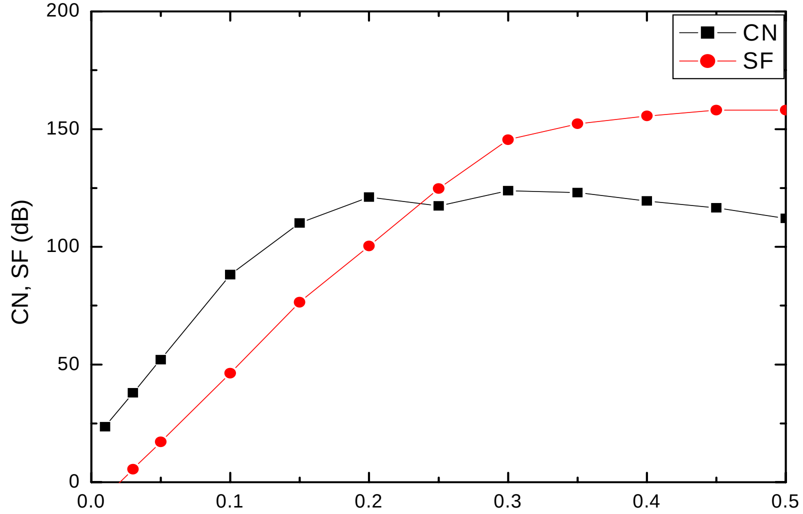

Field Pressure

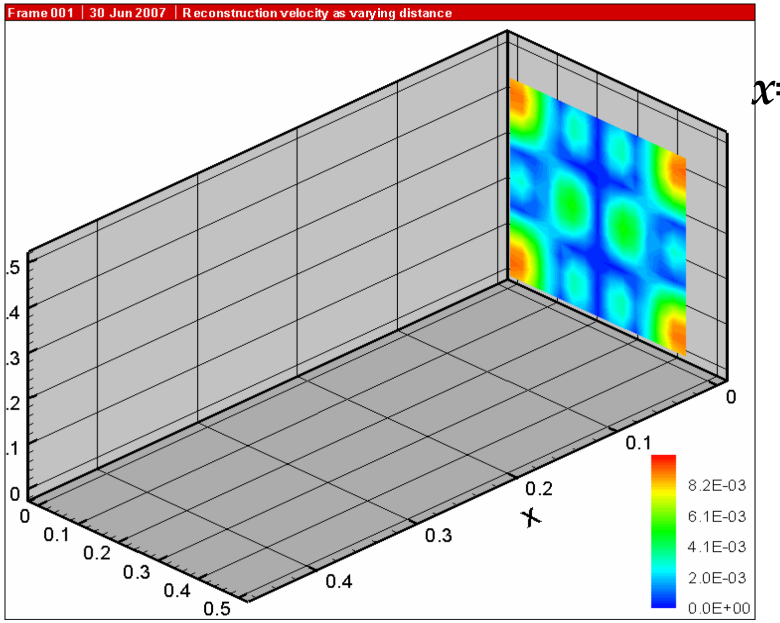

$x = d/\lambda$

Reconstructed Image (SNR = 20 dB)

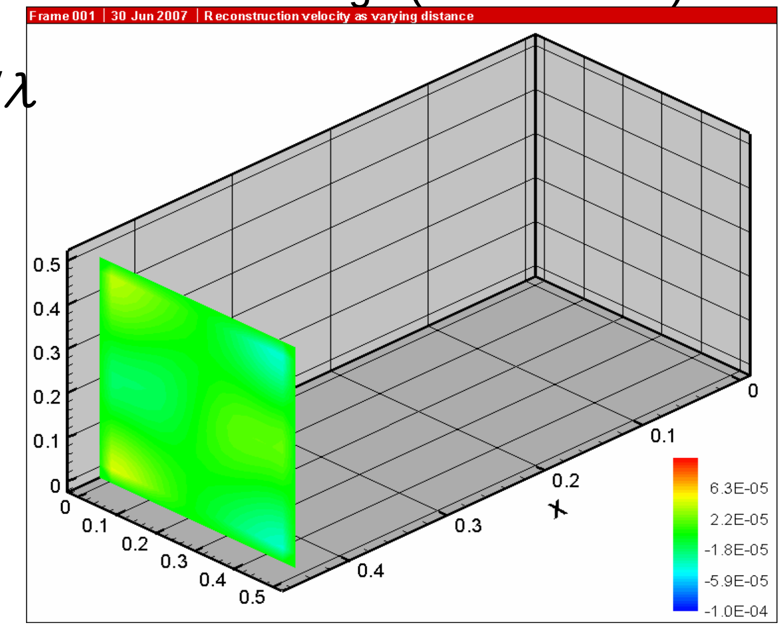

Need of NAH Using the Inverse BEM

- *Why "NAH using the inverse BEM"?*
  - Recent advances in multi-channel data acquisition & signal processing techniques and in computer speed and memory size
  - **Curved source surface: convex/concave/irregular shape**
  - **Light-weight, thin, hot, soft, and other intricate surfaces**
  - **Various boundary conditions incl. open aperture**
  - **Ease in forward prediction by using nearly the same method with the inverse calculation**
  - No special pre-treatment on the source surface

Nonregular-shaped Vibro-acoustic Sources

- Vibro-acoustic sources having complicated surface shapes

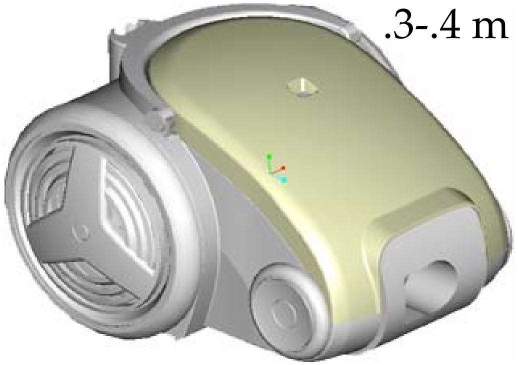

.3-.4 m

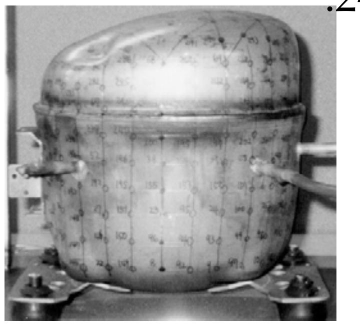

.2-.3 m

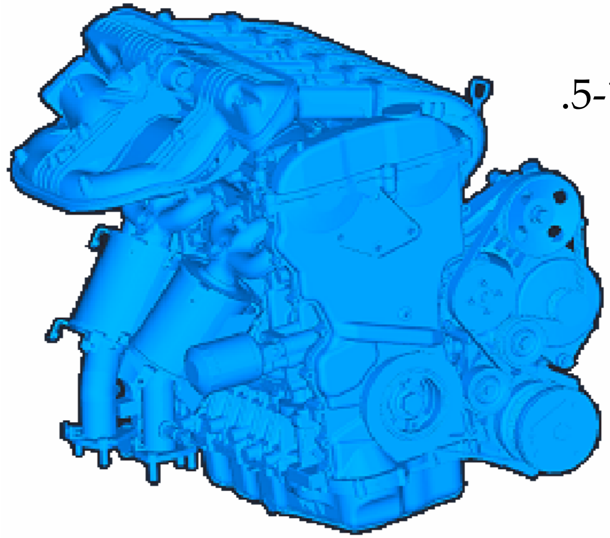

.5-1.0 m

1.3-3 m

O(10^1 m)

(adapted from Williams, et al., JASA)

KAIST

Short History 1

❖ Short history of BEM-based NAH

- **NAH: Progresses in Ultrasonic imaging, Tomography, Digital image enhancement, and other fields**
- Williams, Maynard, Lee (1980, 1985): *Development of spatial F/T based NAH*
- Maynard (1988): *Holography for wideband, odd-shaped noise sources*
- Gardner & Bernhard (1987): *Basic concept of BEM-based NAH*
- Veronesi & Maynard (1989)
  - Singular value decomposition (SVD) to decompose source and field properties into wave-vector domain
- Bai (1992)
  - Formulation of generalized holography equation using direct BEM
- Kim & Ih (1997)
  - Application to car interior / wave-vector filtering
  - Optimal selection of measurement points by EfI method

KAIST

Short History 2

❖ Historical review of BEM-based NAH

- Williams, *et al.* (2000): *Application to airplane interior*
- Zhang, *et al.* (2000)
  - NAH based on the indirect BEM
- Kang & Ih (2000,2001)
  - Nonsingular BEM-based NAH / Use of partially measured data
- Seybert (2002): *Application to aeroacoustic sources*
- Wu, *et al.* (2002)
  - Helmholtz equation least-squares (HELS) method combined with the BEM-based NAH
- Roozen, *et al.* (2004): *BEM-based NAH using EfI method*
- Jeon & Ih (2005)
  - BEM-based NAH combined with the equivalent source technique
- And many other important contributions in recent days ...

Basic Theory of NAH Using the BEM-1

- Kirchhoff-Helmholtz Integral Equation

$$c(\mathbf{r})p(\mathbf{r}) = \int_{S_O} \{ G(\mathbf{r},\mathbf{r_o}) \frac{\partial p(\mathbf{r_o})}{\partial n(\mathbf{r_o})} - \frac{\partial G(\mathbf{r},\mathbf{r_o})}{\partial n(\mathbf{r_o})} p(\mathbf{r_o}) \} \, dS(\mathbf{r_o})$$

- Matrix/Vector Equations $(\mathbf{G_v} = transfer\ matrix)$

$$\mathbf{p_f} = \mathbf{D_f}\,\mathbf{p_s} + \mathbf{M_f}\,\mathbf{v_s}\ ,\quad subject\ \ to\ \mathbf{D_s}\,\mathbf{p_s} = \mathbf{M_s}\,\mathbf{v_s}$$

$$\Rightarrow\ \mathbf{p_f} = (\mathbf{D_f}\,\mathbf{D_s^{-1}}\mathbf{M_s} + \mathbf{M_f})\,\mathbf{v_s} \equiv \mathbf{G_v}\mathbf{v_s}$$

$$(\ SVD\ of\ G\ :\ \mathbf{G_v} = \mathbf{U_v}\,\Lambda_\mathbf{v}\,\mathbf{W_v^H}\ )$$

- Inverse Imaging ($(\ldots)^+$=pseudo-inverse)

$$\mathbf{v_s} = (\mathbf{G_v^H}\mathbf{G_v})^{-1}\mathbf{G_v^H}\,\mathbf{p_f} = \mathbf{G_v^+}\,\mathbf{p_f} = \mathbf{W_v}\,\Lambda_\mathbf{v}^{-1}\,\mathbf{U_v^H}\,\mathbf{p_f}$$

- *Ill-posed Inverse Problem Due to Ill-conditioned System Matrix*

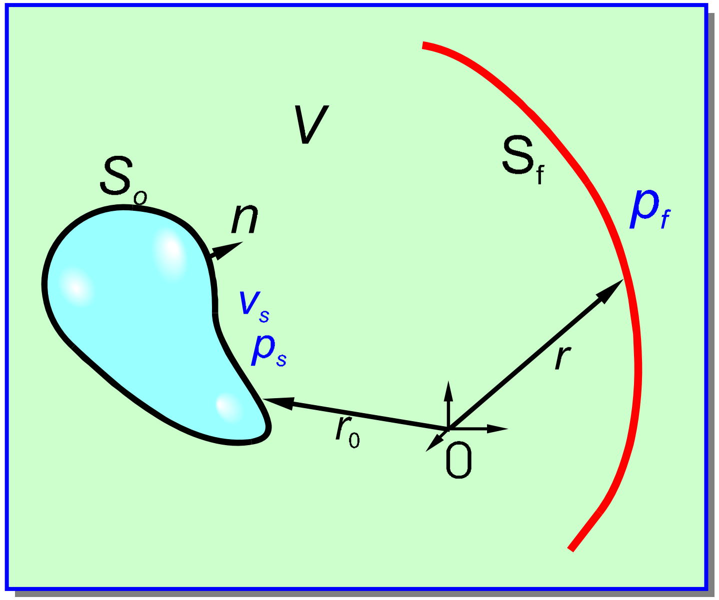

KAIST

Standard Procedure of NAH-BEM-1

Transfer matrix from BE model

$$\mathbf{p}_f = \mathbf{D}_f \mathbf{p}_S + \mathbf{M}_f \mathbf{v}_S$$
$$\equiv \mathbf{G}_v \mathbf{v}_S$$

$$\mathbf{D}_S \mathbf{p}_S = \mathbf{M}_S \mathbf{v}_S$$

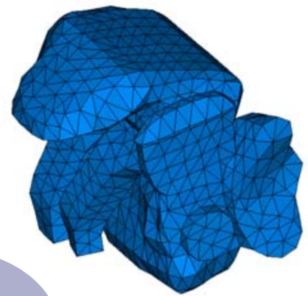

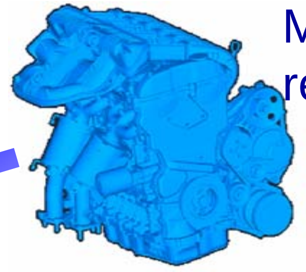

Model reduction

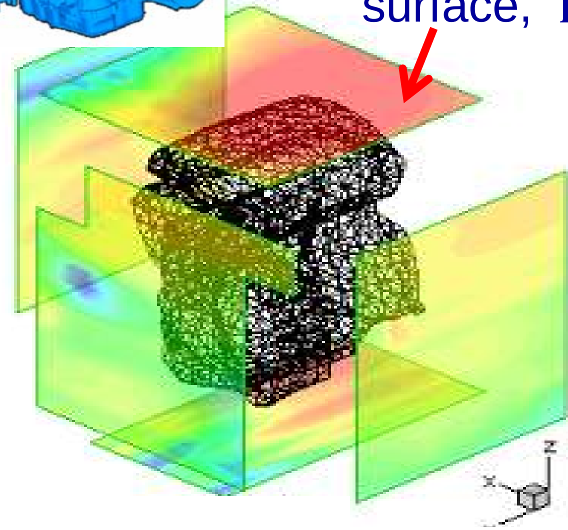

Hologram surface, $\mathbf{p}_f$

Acoustical holography

$$\mathbf{v}_S = \mathbf{G}_v^{+} \mathbf{p}_f$$

Image enhancement by regularization

$$\hat{\mathbf{v}}_S = \mathrm{W} F_l \Lambda^{-1} \mathrm{U}^H \tilde{\mathbf{p}}_f$$

$*F_l$: Wave-vector Filter

Source reconstruction $(\mathbf{v}_S, \vec{I}, p_s)$

Forward field prediction $(\mathbf{v}_f, \vec{I}, \mathbf{p}_f, \mathbf{P}_{rad})$

Source power

$$*F_l = diag(1-(\beta\Lambda_1^2)^{l+1}, \cdots, 1-(\beta\Lambda_n^2)^{l+1})$$

KAIST

Meaning of Decomposed Vibro-acoustic TF

$$\mathbf{p_f} = (\mathbf{D_f}\,\mathbf{D_s^{-1}}\mathbf{M_s} + \mathbf{M_f})\,\mathbf{v_s} \equiv \mathbf{G_v}\mathbf{v_s}$$

Vibro-acoustic transfer matrix

$$\Rightarrow \mathbf{v_s} = (\mathbf{G_v^H}\mathbf{G_v})^{-1}\mathbf{G_v^H}\,\mathbf{p_f} = \mathbf{G_v^+}\mathbf{p_f} = \mathbf{W_v}\,\Lambda_v^{-1}\,\mathbf{U_v^H}\,\mathbf{p_f}$$

Normal velocity of vibrating source

Sound pressure at hologram surface

$$\mathbf{U^H U = I}$$
$$\mathbf{W^H W = I}$$
$$\mathbf{\Lambda_v} = \begin{bmatrix} \Lambda_1 & 0 & \dots \\ 0 & \Lambda_2 & \dots \\ . & . & \dots \end{bmatrix}$$

$$(SVD\ \ of\ \ G : \mathbf{G_v} = \mathbf{U_v}\Lambda_v\mathbf{W_v^H})$$

Projection vector:
Propagating wave mode from acoustic field to measurement field

Conversion factor:
Contribution of each radiating wave mode to propagating sound

Projection vector:
Radiated wave mode from surface vibration to acoustic field

KAIST

BEM-based NAH: *Backward* Calculation w/o Regularization

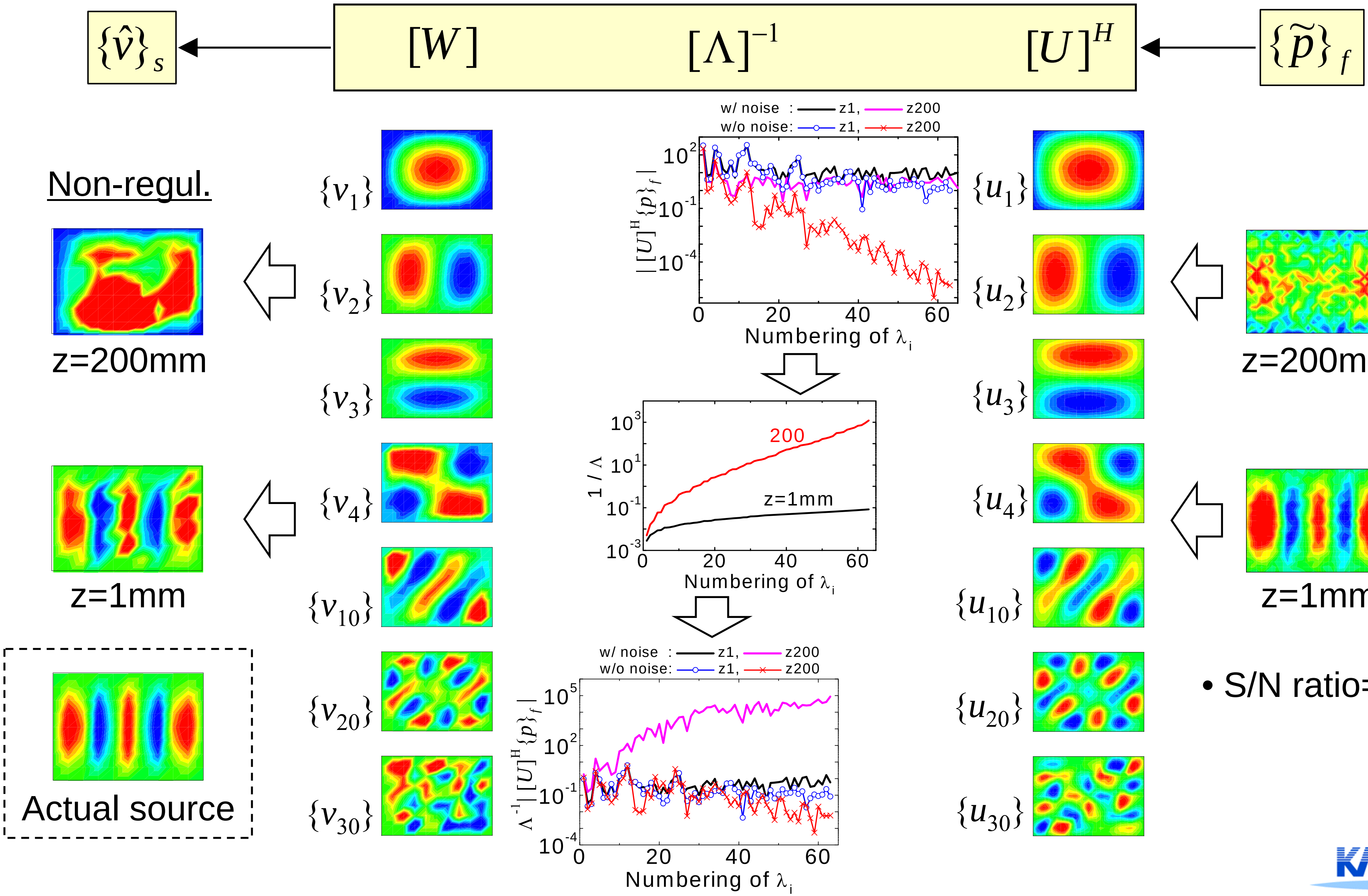

- S/N ratio=30

Ill-posed Nature of Backward Reconstruction

- Instability Due to High Condition Number
- Improvement of Reconstructed Image by an Effective Suppression of High-order Wave Vectors

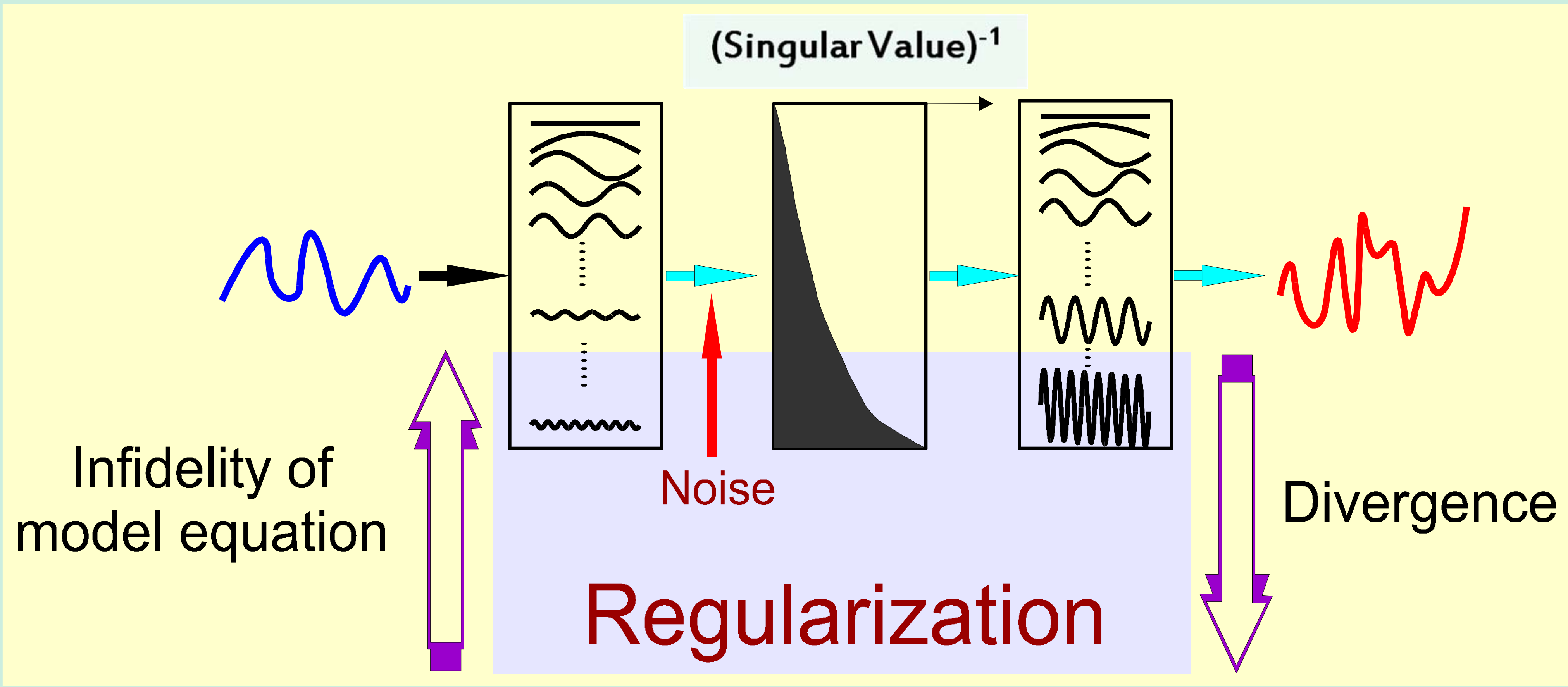

- **How to determine** optimal regularization order?

Short History 1

❖ Short history of regularization in BEM-based NAH

- **Progresses in Inverse theory, Ultrasonic imaging, Tomography, Digital image enhancement, and other fields → Regularization in NAH** (Ref. AN Tikhonov and VY Arsenin, *Solutions of Ill-posed Problems*, Halsted Press, New York, 1977; HC Andrews and BR Hunt, *Digital Image Restoration*, Prentice-Hall, Englewood Cliffs, 1977; PC Hansen, *Rank-Deficient and Discrete Ill-Posed Problems*, SIAM, Philadelphia, 1998; A Kirsch, *An Introduction to the Mathematical Theory of Inverse Problems*, Springer-Verlag, New York, 1996; EG Williams, *Fourier Acoustics*, Academic Press, London, 1999; etc.)
- Fleischer and Axelrad (1986): *Wiener filtering for field image enhancement*
- Lee and Sullian (1988): *Resolution enhancement by field extrapolation*
- Demoment (1989): *Overview (IEEE)*
- Biemond (1990): *Iterative method*
- Photiadis (1992): *SVD for wave vector filtering*
- Kim & Ih (1996): *Optimal wave-vector filtering*

KAIST

Short History 2

❖ Short history of regularization in BEM-based NAH

- Nelson & Yoon (2000): *Generalized cross-validation technique*
- Kim & Ih (2000): *Design of optimal wave vector filter*
- Williams (2001): *Morozov discrepancy principle*
- Valdivia and Williams (2005): *Krylov subspace iterative methods*
- And many others …

Image Enhancement by Regularization

- Regularization (Filtering)
  - Empirical truncation method
  - Tikhonov method (use of regularization parameter)
  - Landweber iteration method, etc.

- Hot Point:
  - Determination of optimal discarding order, *or*
  - Determination of optimal wave vector filter shape

- Searching method for optimal parameters
  - Mean-square error estimation using variance (Morozov)

    ... *Use of trade-off relation between bias and random errors*
  - Use of generalized cross validation (GCV) technique
  - L-curve criterion, Genetic algorithm, etc.
    - *Truncation of singular values (TSV)*
    - *Regularization parameter (RP)*
    - *Termination of iteration process (TIP)*

TIP: *Optimal wave-vector filter coefficients*

- **Pseudo-inverse solution *without filtering***

$$\hat{v}_s = W\, diag(\Lambda_1, \ldots\ldots, \Lambda_n)^{-1} U^H \tilde{p}_f$$

- **Pseudo-inverse solution *with filtering***

$$\hat{\mathbf{v}}_s^l = \mathbf{W}\mathbf{F_l}\, diag(\Lambda_1, \Lambda_2, \ldots, \Lambda_n)^{-1} \mathbf{U^H}\tilde{\mathbf{p}}_\mathbf{f}$$

or $$\hat{\mathbf{v}}_\mathbf{s} = \mathbf{W}\, diag\left(\frac{1-\left(1-\beta\Lambda_1^2\right)^{l_{opt}+1}}{\Lambda_1}, \ldots, \frac{1-\left(1-\beta\Lambda_n^2\right)^{l_{opt}+1}}{\Lambda_n} \right) \mathbf{U^H}\tilde{\mathbf{p}}_\mathbf{f}$$

- **Optimal wave-vector filter (*i.e., filter coefficients*)**

$$F_l = diag\left[1-\left(1-\beta\Lambda_1^2\right)^{l_{opt}+1}, \ldots, 1-\left(1-\beta\Lambda_n^2\right)^{l_{opt}+1}\right]$$

Ex: *Designed optimal wave-vector filters*

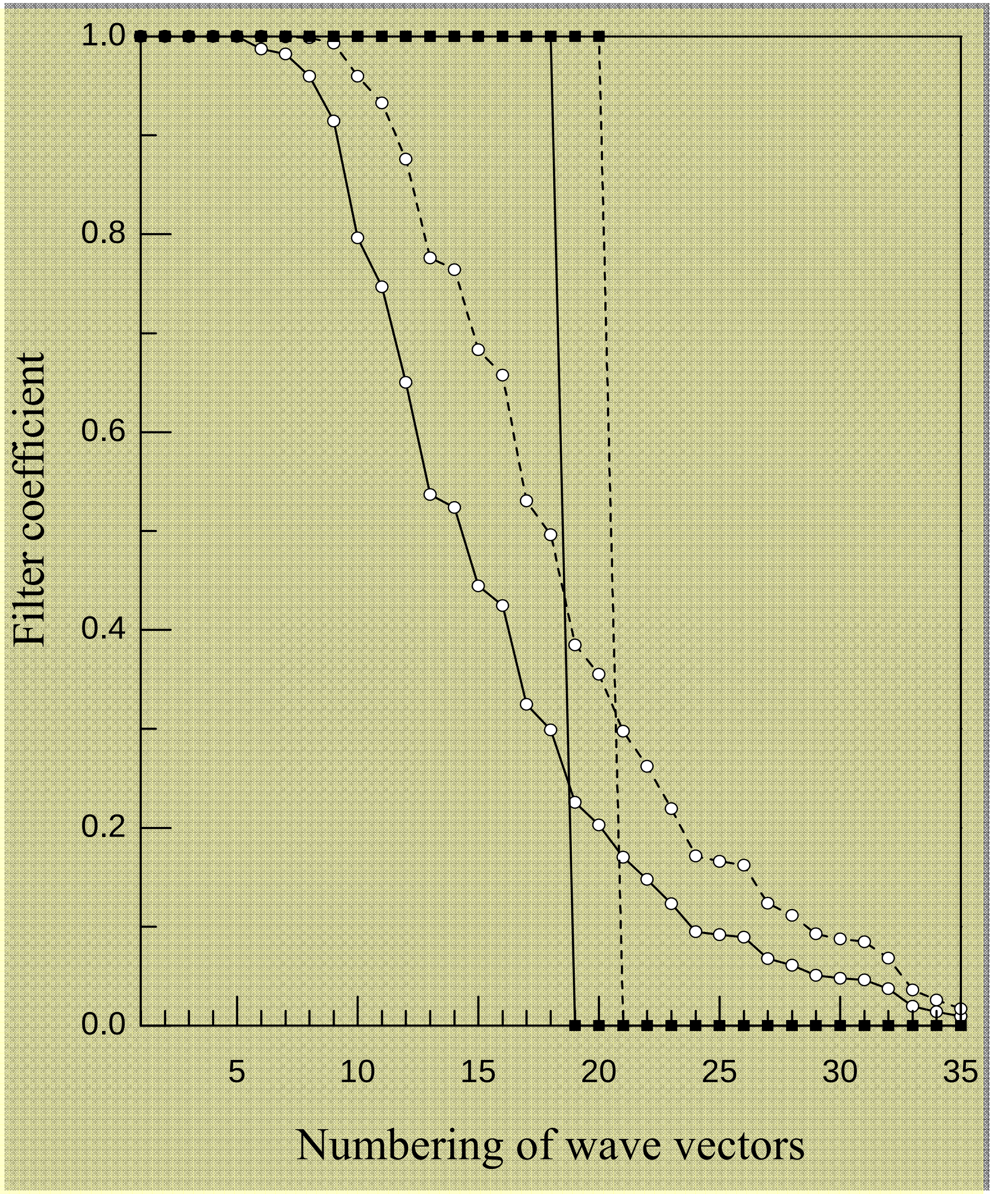

Shapes of the optimal wave-vector filters for regularization

Truncation method

111.5 Hz

270.3 Hz

Iteration method

111.5 Hz

270.3 Hz

BEM-based NAH: *Backward Calculation w/ Regularization*

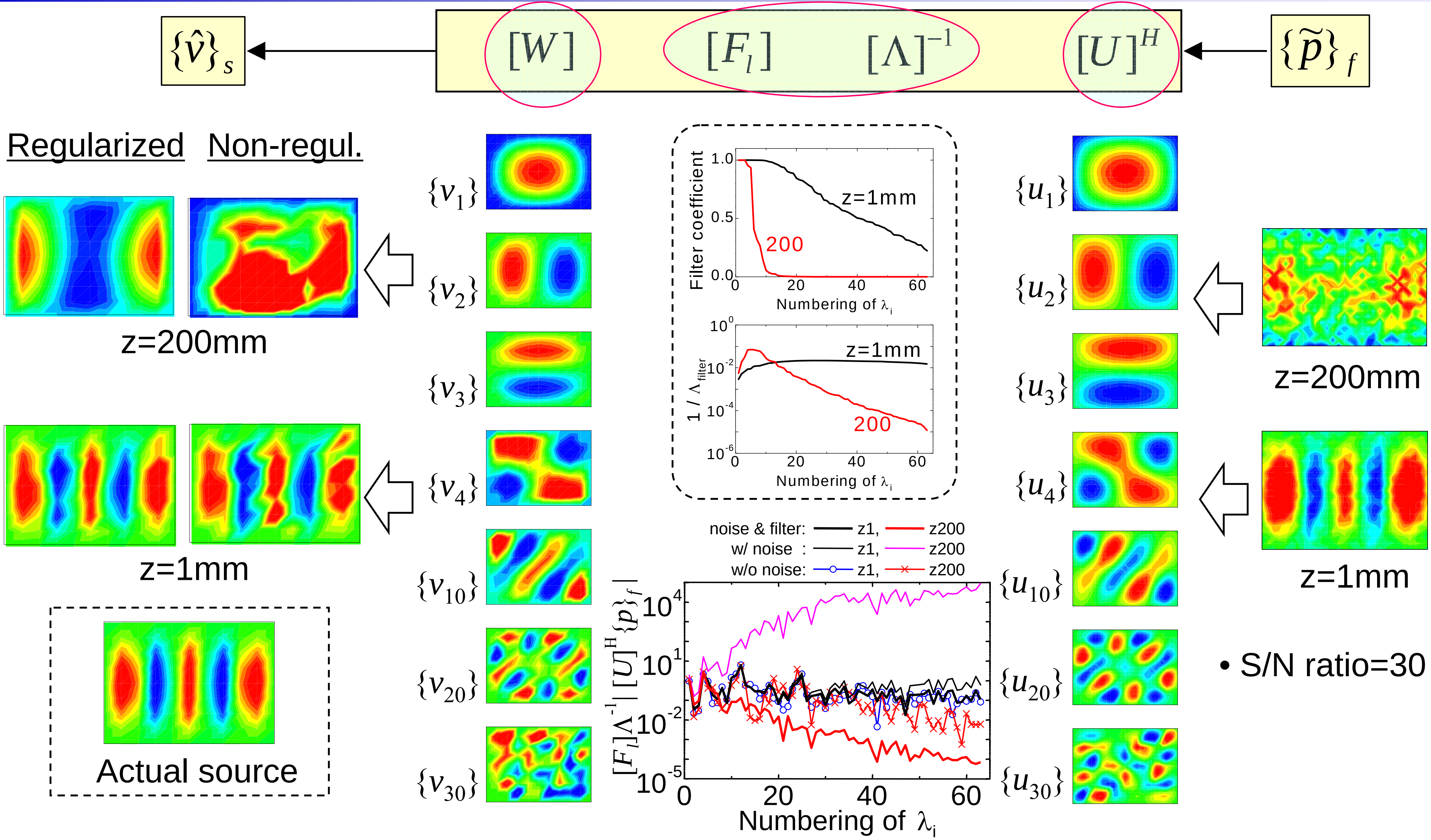

Post Processing – *Surface and Forward Field Data*

- **Calculation of acoustical field parameters:**
  - Surface normal acoustic intensity
    Active and reactive intensity ... $\vec{I} = \langle \overline{p \cdot \vec{u}} \rangle$
  - Acoustic normal impedance on the source surface ... $\tilde{z} = \left(\frac{p}{u} \right)$
  - Radiated sound power ... $\Pi_{Rad} = \iint_S \vec{I} \cdot \vec{n} dS$
  - Radiation efficiency ... $\sigma_{rad} = \iint_S \vec{I} \cdot \vec{n} dS \Big/ S \langle \overline{v_n^2} \rangle \rho_0 c_0$
- **Forward prediction:**
  - Sound pressure and particle velocity at field points
  - Directivity pattern, $Q(\theta)$
  - Field sound intensity vector, $\vec{I}$

Example: IC Engine (I. BE modeling & measurement)

❖ BE model & measurement points

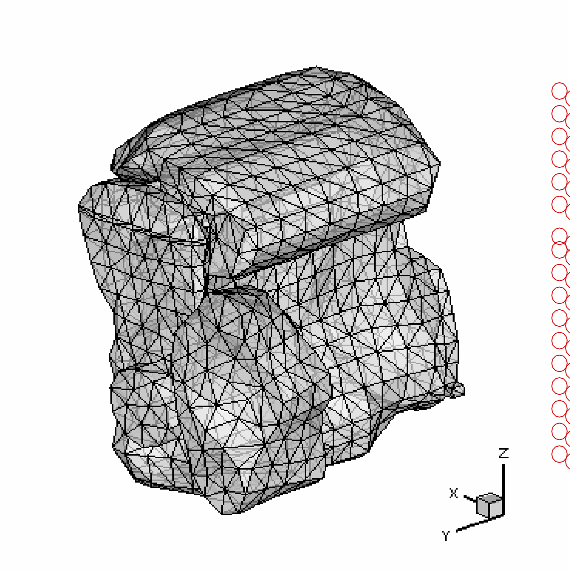

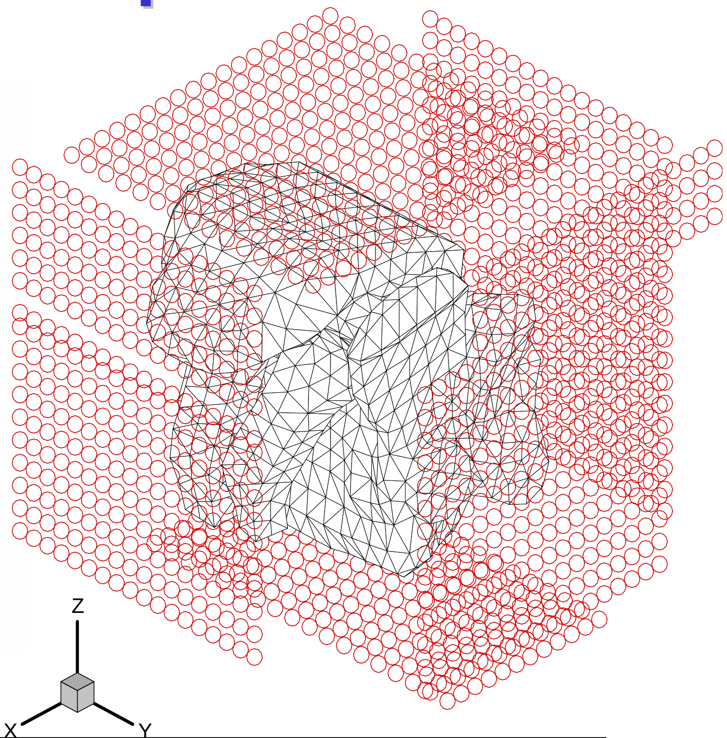

No. of surface nodes (*n*)	1076
No. of surface elements	2148
Characteristic length	98.03 mm
Frequency cutoff	$f_{max} < 580$ Hz
No. of measurement points (*m*)	1440
Microphone spacing	50 mm

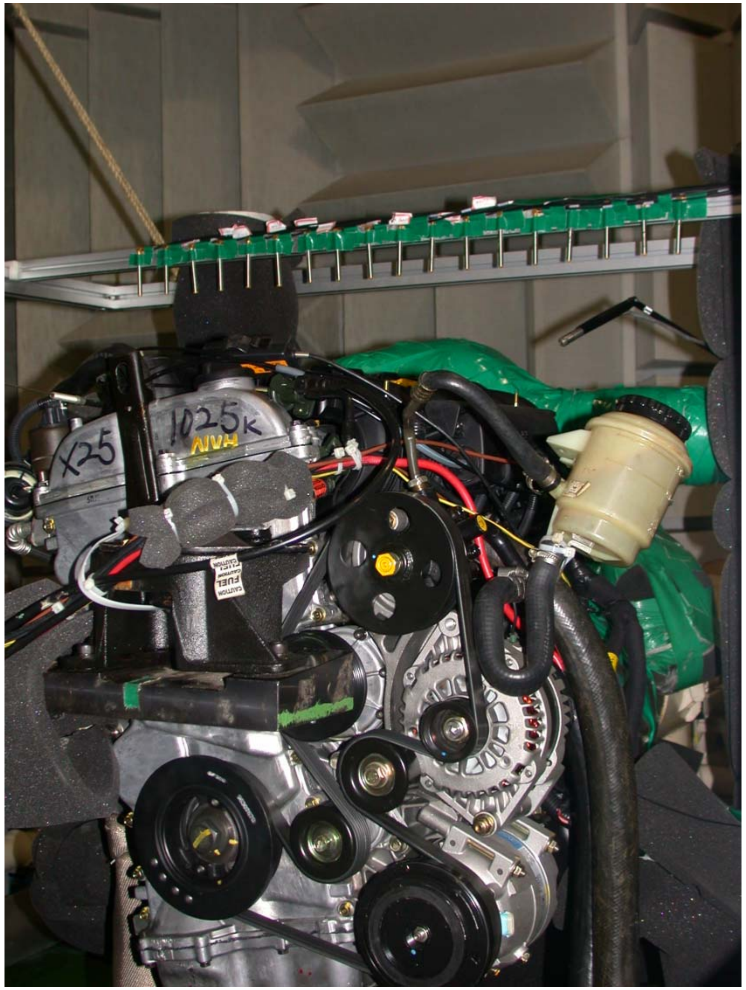

Dimension:
729(l)x625(w)x693(h) mm^3

Example: IC Engine (II. Regularization)

❖ Measured pressure and regularization

- **Measured pressure contour**

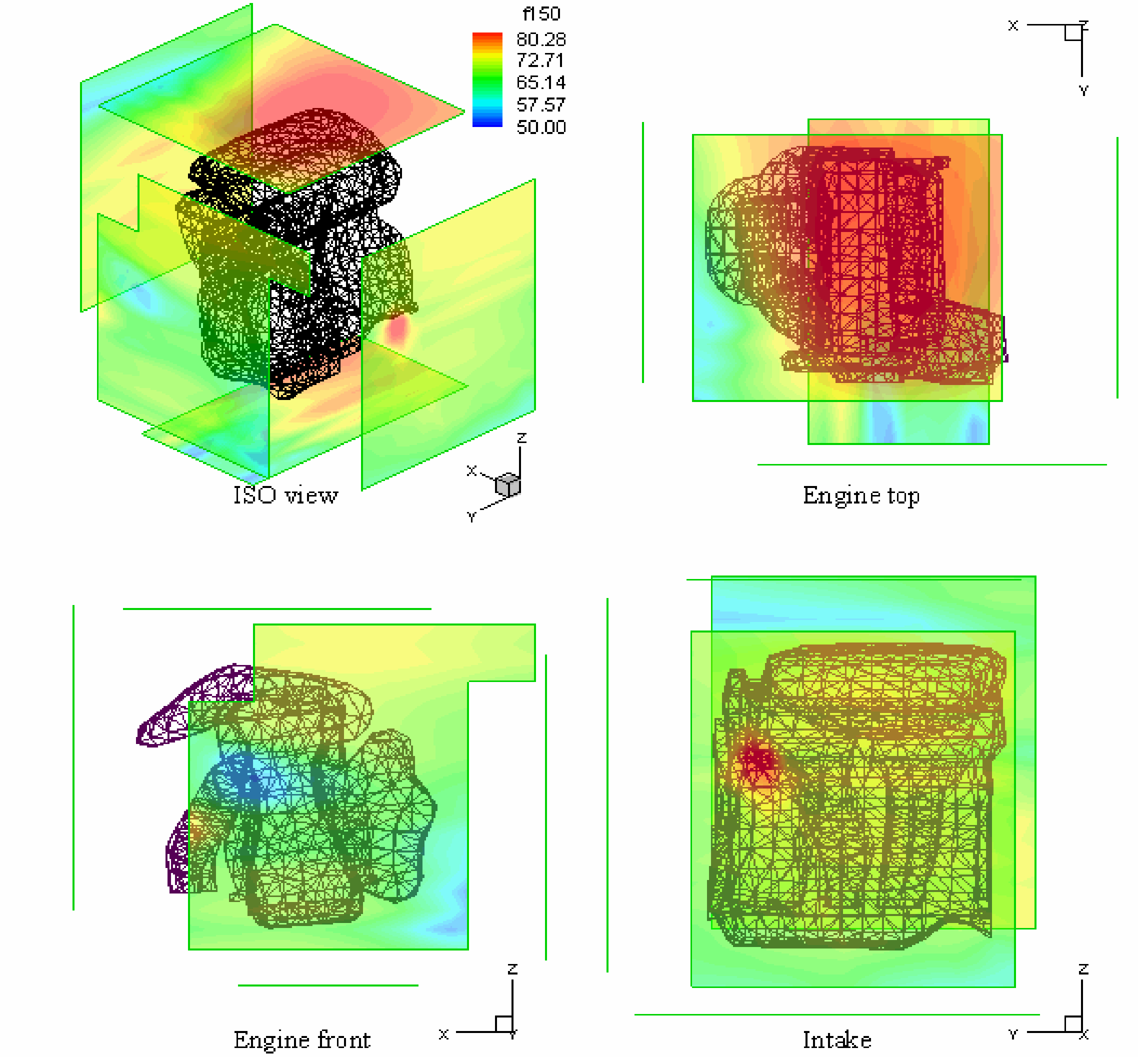

- **Regularization**
  - Iterative regularization
  - GCV function for a parameter selection

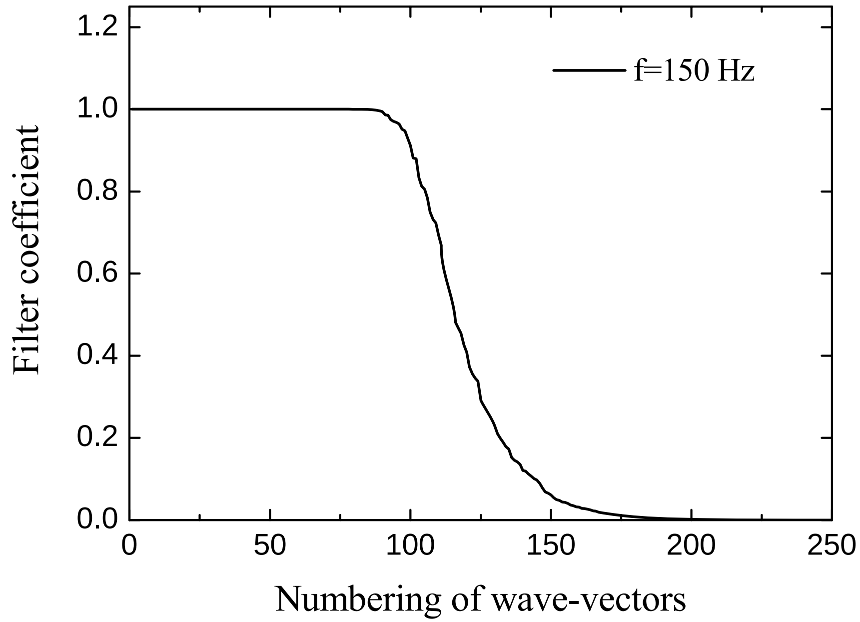

KAIST

Example: IC Engine (III. Post processing)

Surface intensity at ***3000 rpm***

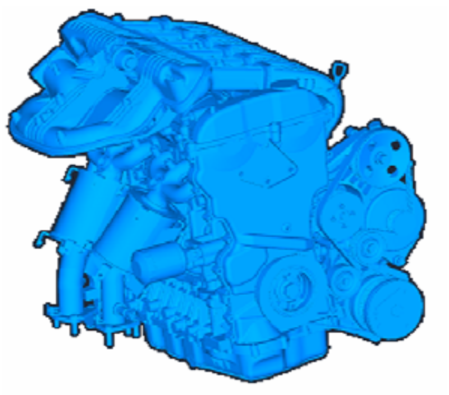

150 Hz

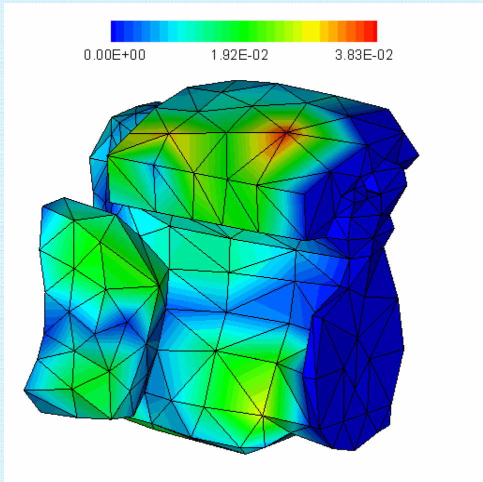

200 Hz

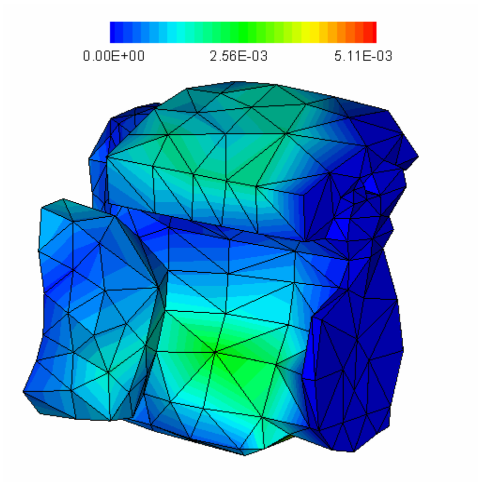

Frequency sweep

3000 rpm

Animation of surface velocity field

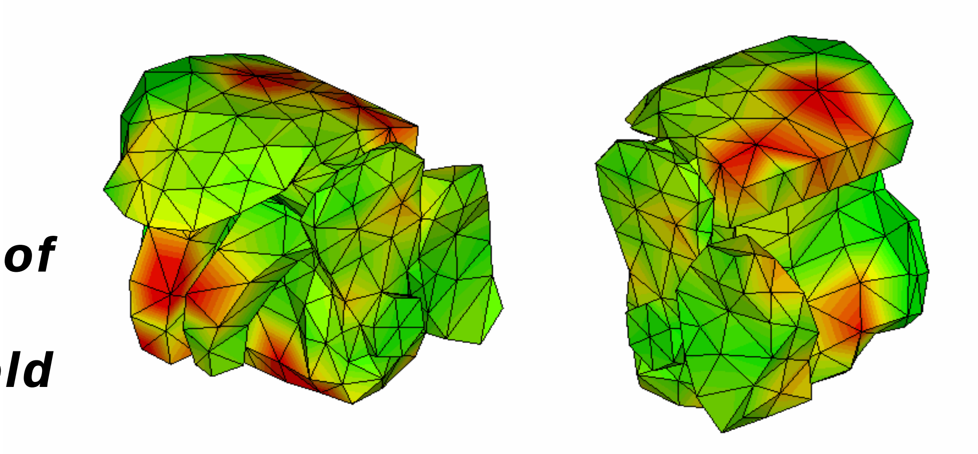

Example: IC Engine (IV. Post processing–Directivity)

❖ Directivity of radiation at 1 m position (3000 rpm)

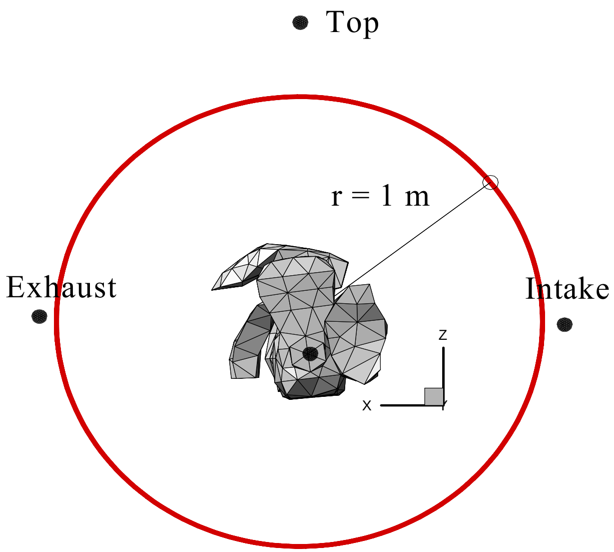

f=100 Hz

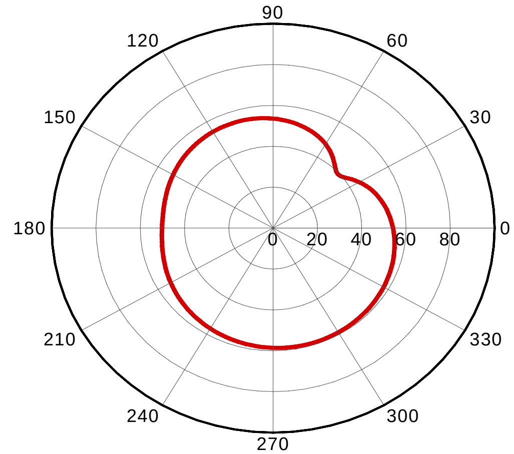

f=150 Hz (3rd order)

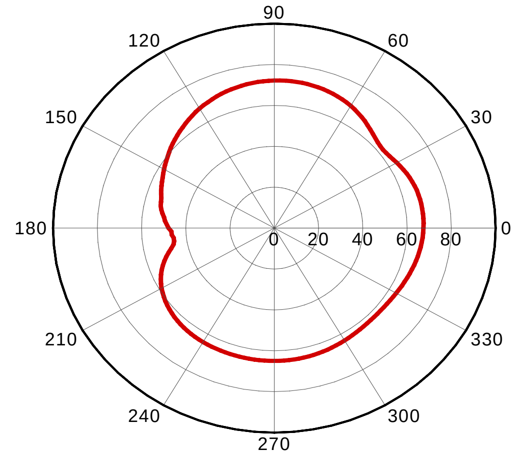

f=200 Hz

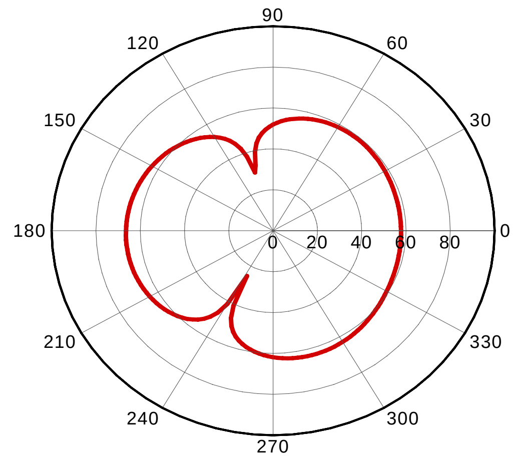

f=350 Hz (6th order)

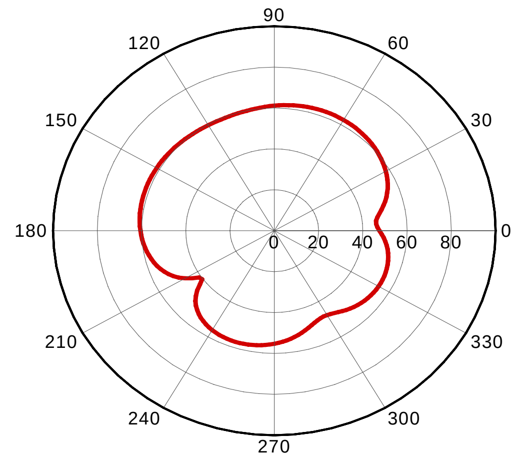

Example: IC Engine (V. Post processing–Radiated Power)

❖ **Power** contribution from each part (f_c=157 Hz in 1/3-octave band)

1000 rpm

2000 rpm

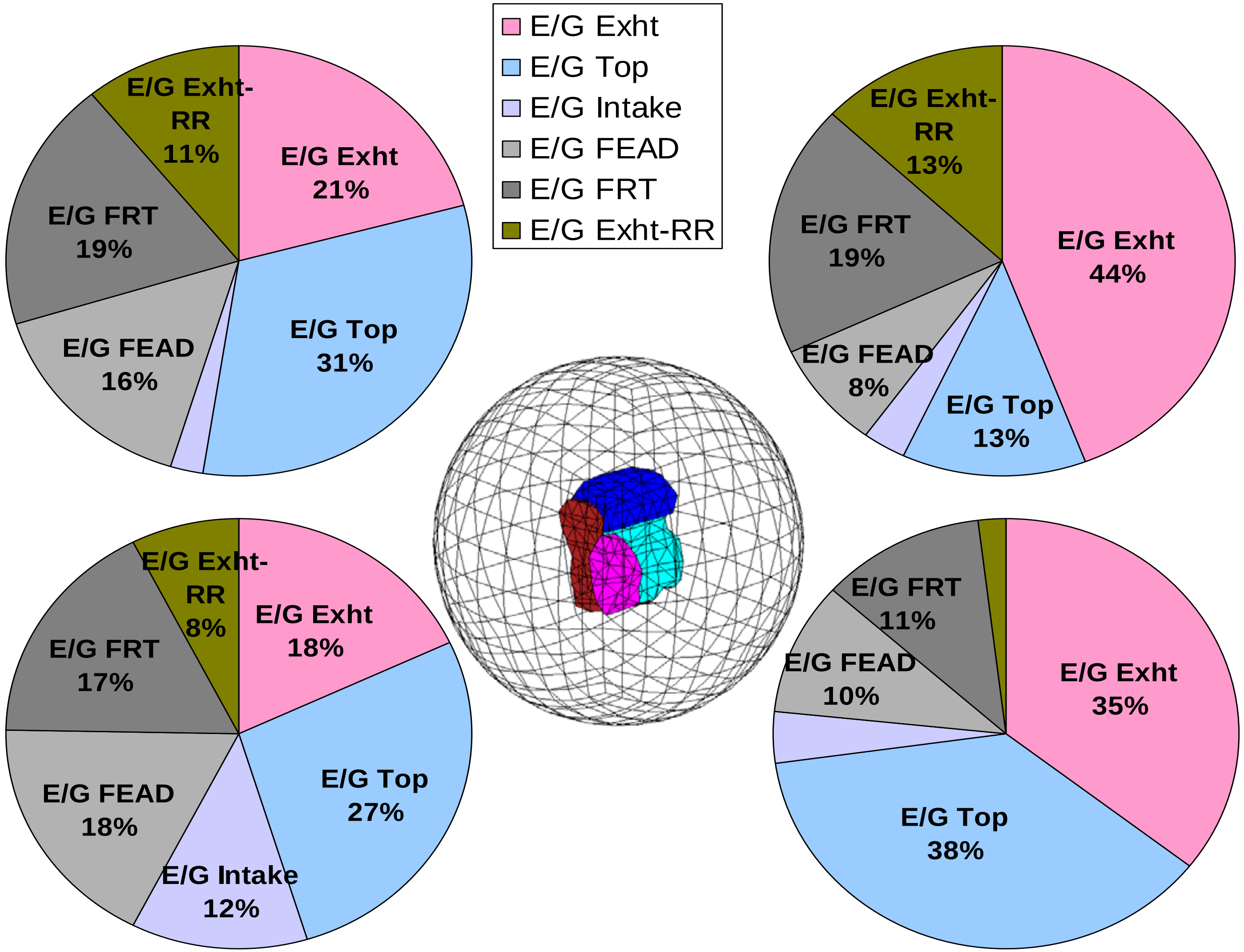

3000 rpm

4000 rpm

Further Study Topics in BEM-based NAH

- Fast and stable method in determining sensor positions
- Precise measurement technique
- New measurement technique for dealing with practical problems: (ex) patch holography
- Quick measurement and processing of field data
- Design of optimal wave vector filter for regularization
- Underdetermined NAH problems
- Adoption of fast algorithm in boundary element calculations
- Treatment of repetitive transient sound
- Measurement of vectorial quantity in the hologram plane
- Reconstruction of structural wave field
- Reconstruction of rotating source field
- Scattering problems
- Extension of application area
- etc.

KAIST

Measurement and Calculation Efforts

❖ Problems in applying the inverse BEM tech.

- **Calculation effort**

No. of BE nodes

$$T_{Construction}(\mathbf{G}_{v}),\ T_{Solve}(\mathbf{G}_{v}^{+}) \sim O(n^{3})$$

- **Measurement effort**
  - number of measurements ≥ number of BE nodes

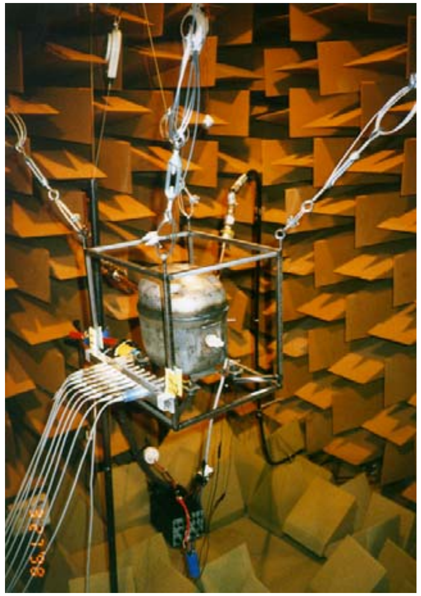

- **Ex: Total NAH realization time for an engine (w/ regularization)**
  - For a single RPM, 100 frequencies (P4, 2G)

	E/G BE 1 (Fine)	E/G BE 2 (Rough)
Nodes	1076	329
Measurements	1440	369
Measurement effort	8 hours	4 hours
Overall calc. effort	64 hours	2 hours
Frequency limit	875 Hz	470 Hz

Use of Equivalent Source Method for NAH

❖ Generalized ESM (w/ multi-point multipoles)

- **Approximated solution with *E* multipole sources of order *J***

$$p_f(\mathbf{r}_m,\omega)=\sum_{e=1}^{E}\sum_{j=1}^{J}C_j^e\psi_j(\mathbf{r}_m-\mathbf{r}_e,\omega)$$

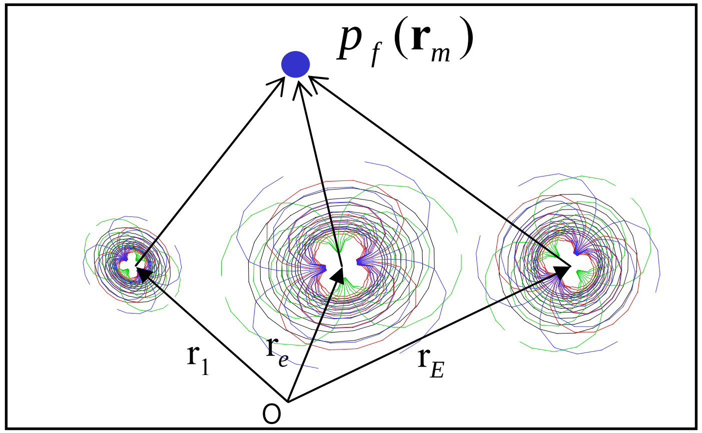

- **Matrix form for *M* measurements**

$$\begin{bmatrix} p_f(\mathbf{r}_1,\omega) \\ \vdots \\ p_f(\mathbf{r}_M,\omega) \end{bmatrix}_{M\times 1} = \begin{bmatrix} \psi_1^{11} & \cdots & \psi_1^{1E} \\ \vdots & \ddots & \vdots \\ \psi_1^{M1} & \cdots & \psi_1^{ME} \end{bmatrix}_{M\times E} \begin{bmatrix} C_1^1 \\ \vdots \\ C_1^E \end{bmatrix}_{E\times 1} + \cdots + \begin{bmatrix} \psi_J^{11} & \cdots & \psi_J^{1E} \\ \vdots & \ddots & \vdots \\ \psi_J^{M1} & \cdots & \psi_J^{ME} \end{bmatrix}_{M\times E} \begin{bmatrix} C_J^1 \\ \vdots \\ C_J^E \end{bmatrix}_{E\times 1}$$

$$= \begin{bmatrix} \mathbf{\Psi}_1 & \cdots & \mathbf{\Psi}_J \end{bmatrix}_{M\times Q} \begin{bmatrix} \mathbf{C}_1 \\ \vdots \\ \mathbf{C}_J \end{bmatrix}_{Q\times 1}$$

M x Q spherical function matrix (M ≥ Q)

System equation

$$\mathbf{p}_f = \mathbf{\Psi}_1\mathbf{C}_1 + \cdots + \mathbf{\Psi}_J\mathbf{C}_J = \mathbf{\Phi}\cdot\mathbf{D}$$

(Ph.D. Thesis, IY Jeon, KAIST, 2005)

KAIST

Use of ESM Technique 1

❖ Test example: Canister-type vacuum cleaner

▪ Actual source & BE model

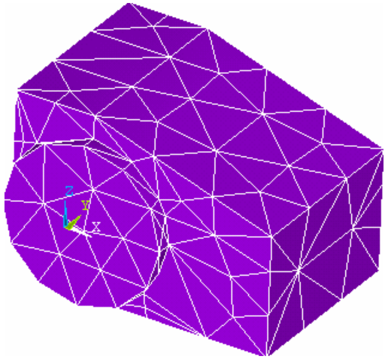

▪ Field pressure spectrum

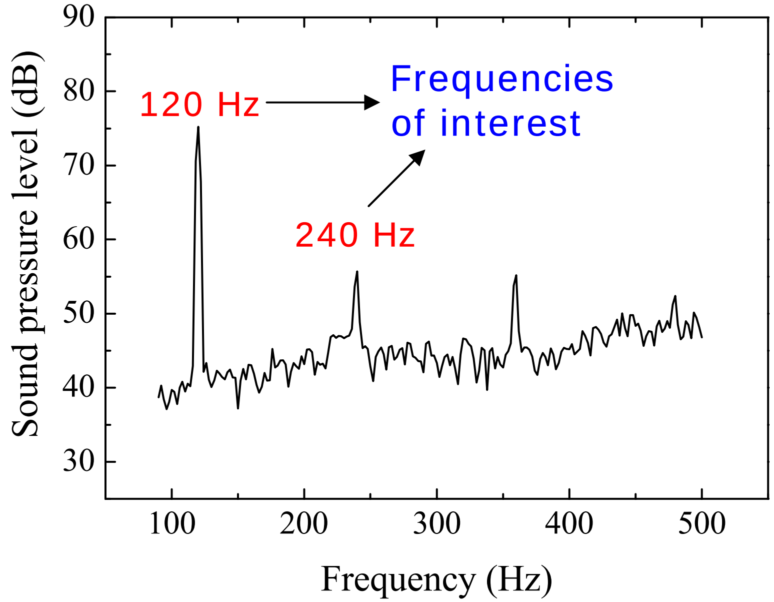

▪ Measuring points

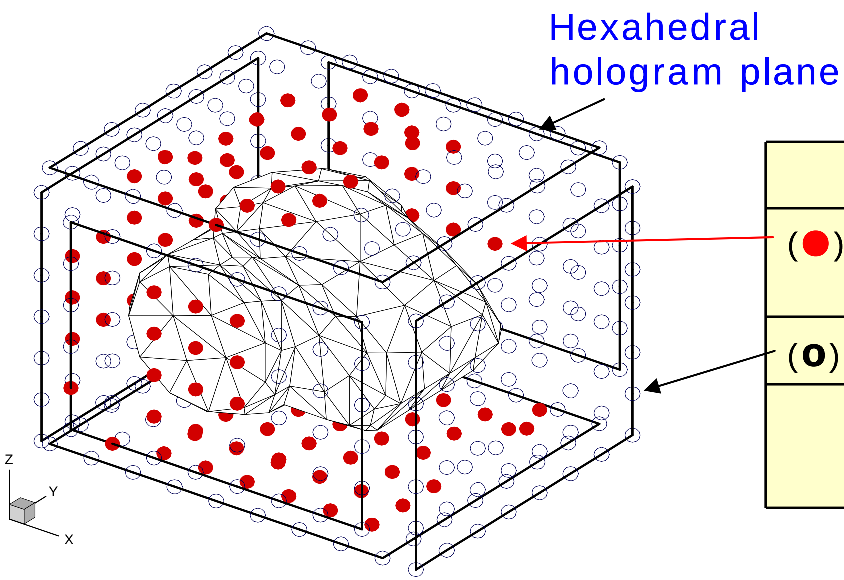

No. of surface nodes (*n*)	170
(●) Measured field points (M_1) selected by the EfI method	**100**
(**o**) Regenerated points (M_2)	252
Characteristic length & frequency limit	78.8 mm (f_{max}<725 Hz)

KAIST

Use of ESM Technique 2

❖ Reconstruction results

- **Reconstruction error**

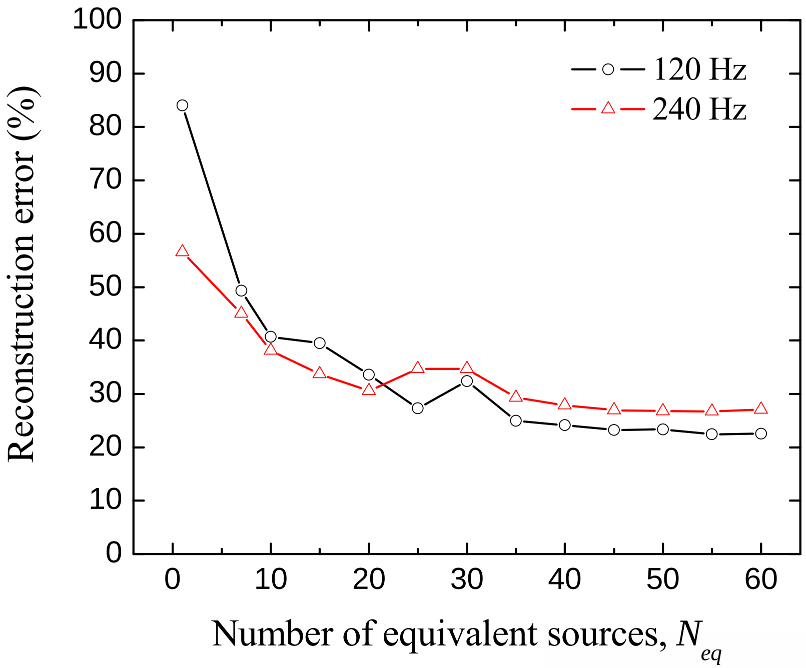

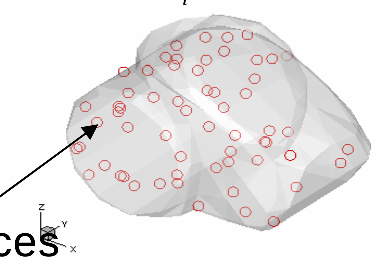

N.B.
Position of equivalent sources inside the actual source were selected by the EfI method

- **Measured sound field**

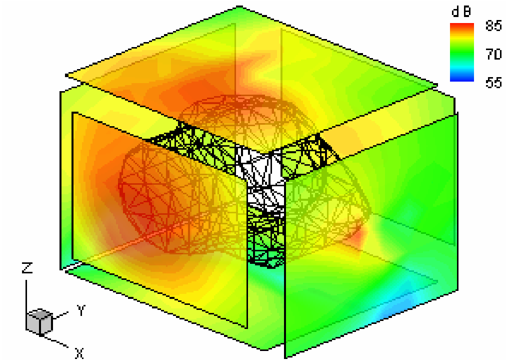

120 Hz

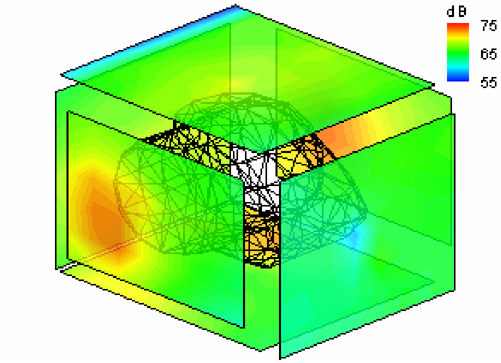

240 Hz

- **Reconstructed sound field (N_{eq}=60)**

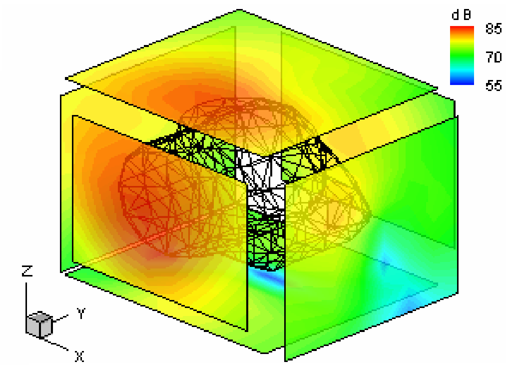

120 Hz
(ε = 23%)

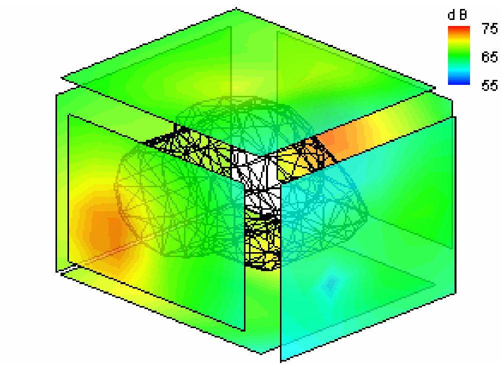

240 Hz
(ε = 27%)

KAIST

Augmentation of Field Data by Additional Reflectors

❖ A rigid reflector is placed at different positions at each measurement, generating independent $[p_f]$'s and $[G]$'s.

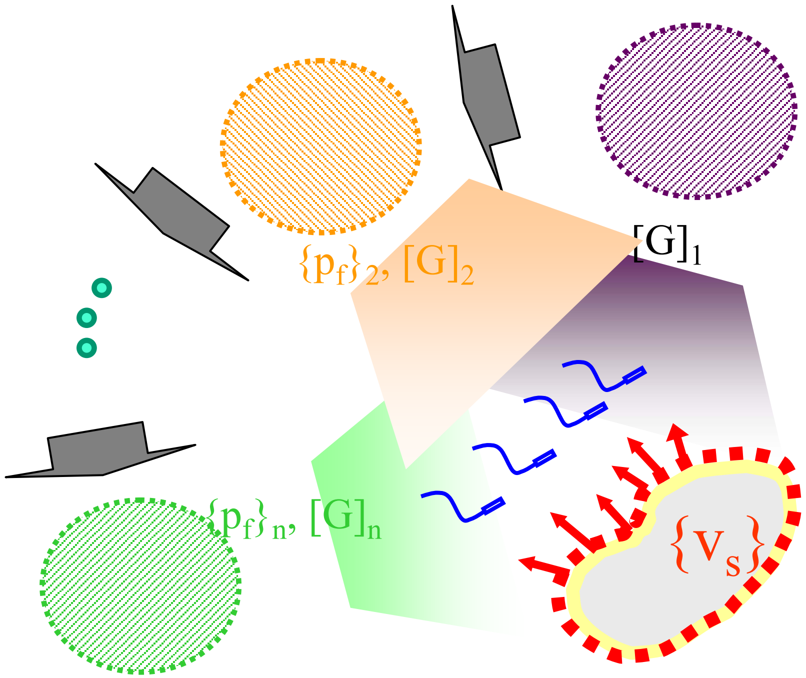

$$[p_f]_1 = [G]_1 \{v_s\}$$
$$[p_f]_2 = [G]_2 \{v_s\}$$
$$\cdots$$
$$[p_f]_n = [G]_n \{v_s\}$$

$$\{v_s\} = \begin{bmatrix} [G]_1 \\ [G]_2 \\ \cdots \\ [G]_n \end{bmatrix}^+ \begin{Bmatrix} \{p_f\}_1 \\ \{p_f\}_2 \\ \cdots \\ \{p_f\}_n \end{Bmatrix}$$

❖ Premise

- The source impedance does not change appreciably by introducing a reflector into a close near-field to the source (Lee & Ih, JSV ,1995)

$$\{v_s\}_1 = \{v_s\}_2 = \cdots = \{v_s\}_n$$

(Ph.D. Thesis, SI Kim, KAIST, 2007)

Inverse Estimation by Beam Tracing 1

❖ TF between p_n (field points) and $p_{s,m}$ (source points)

$$p_n = \boxed{p_{s,m}\frac{e^{j(k+j0.5AF)a_1}}{a_1}} + \boxed{p_{s,m}\frac{e^{j(k+j0.5AF)a_2}}{a_2}r_1(\theta)} + \cdots + \boxed{p_{s,m}\frac{e^{j(k+j0.5AF)a_{nr}}}{a_{nr}}\prod_{i=1}^{nr-1} r_i(\theta)}$$

Direct sound — 1st reflected sound — nth reflected sound

$$p_n = p_{s,m}\underbrace{\left[\frac{e^{j(k+j0.5AF)a_1}}{a_1} + \frac{e^{j(k+j0.5AF)a_2}}{a_2}r_1(\theta) + \cdots + \frac{e^{j(k+j0.5AF)a_{nr}}}{a_{nr}}\prod_{i=1}^{nr-1} r_i(\theta)\right]}_{H_{nm}}$$

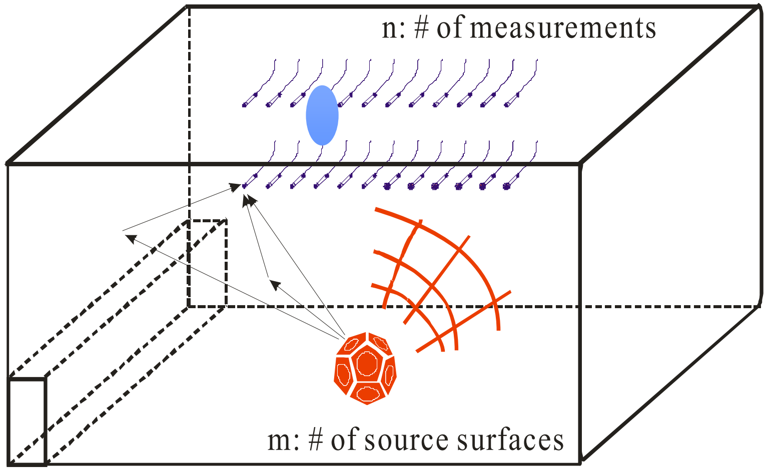

❖ Matrix formulation

$$\begin{Bmatrix} p_1 \\ p_2 \\ \vdots \\ p_n \end{Bmatrix} = \begin{bmatrix} H_{11} & H_{12} & \cdots & H_{1m} \\ H_{21} & H_{22} & \cdots & H_{2m} \\ \vdots & \vdots & \vdots & \vdots \\ H_{n1} & H_{n2} & \cdots & H_{nm} \end{bmatrix} \begin{Bmatrix} p_{s,1} \\ p_{s,2} \\ p_{s,3} \\ \vdots \\ p_{s,m} \end{Bmatrix} \quad or \quad \mathbf{P}_{f,n\times 1} = H_{n\times m}\mathbf{P}_{s,m\times 1}$$

❖ Inversion of acoustic transfer function

$$\mathbf{P}_{s,m\times 1} = H^{\dagger}_{n\times m}\mathbf{P}_{f,n\times 1}$$

(Reconstruction of source pressure field)

Inverse Estimation by Beam Tracing 2

❖ Test example

- Omni-directional source with constant pressure (press. magn. = 0.2)
- 20 elements for source
- Source position: (2.3, 2.36, 1.3)
- Equidistant 24 receivers (4×3×2)
  - Choice of first 20 points

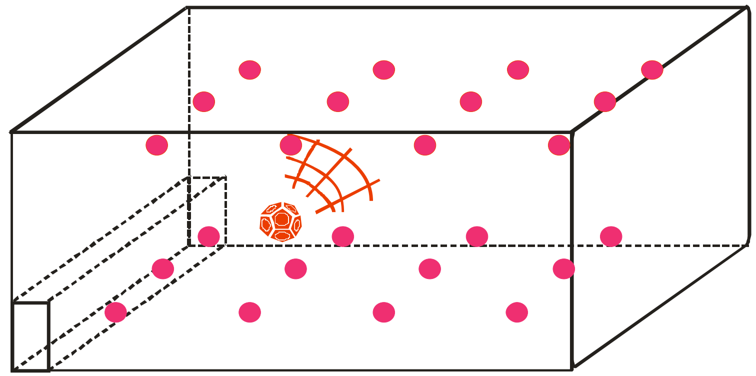

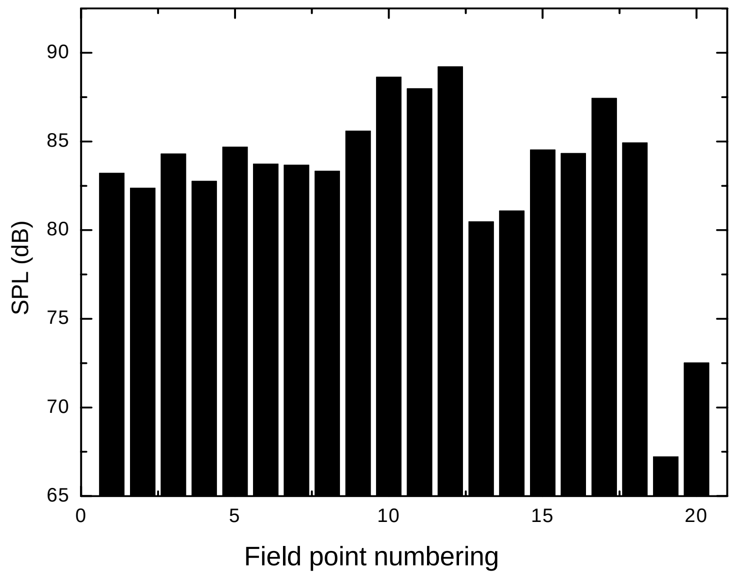

(Reconstruction of source pressure field)

$$\mathbf{P}_{o,m\times1} = H^{\dagger}_{n\times m}\mathbf{P}_{f,n\times1}$$

Without noise

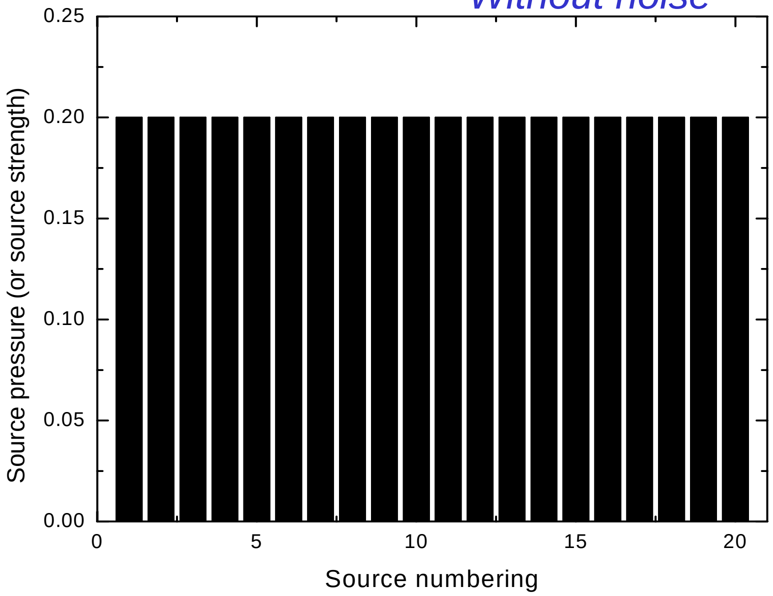

(Ph.D. Thesis, CH Jeong, KAIST, 2007)

KAIST

ACKNOWLEDGMENT

Most of the works in this presentation have been collaborated with the former and current Ph.D. students at the Acoustics Lab. in KAIST as follows:

- *Dr. B.-K. Kim (Korea Inst. of Machinery & Metals, Korea)*
- *Dr. S.-C. Kang (Doosan Heavy Ind. Co., formerly Daewoo Heavy Ind. Co., Korea)*
- *Dr. I.-Y. Jeon (Samsung SDI Co., Korea)*
- *Dr. J.-H. Jeong (Hyundai Motor Co., Korea)*
- *Mr. S.-I. Kim (Samsung Electronics Co., Korea)*
- *Dr. C.-H. Jeong (KAIST)*
- *Mr. A. Oui and Mr. H.-W. Jang (KAIST)*

- *Dr. B.-U. Koo (Agency for Defense & Development, Korea)*
- *Dr. S.-J. Kim (Samsung Electronics Co, formerly at LG Elec. Co., Korea)*

Technical and financial supports from the following companies are acknowledged:

Sound Intensimetry

- **Principle:** *Finite difference approximation*

$$\nabla p \approx \frac{\Delta p}{\Delta r} = \frac{p_2 - p_1}{\Delta r}$$

  - Pressure & velocity: $p \approx \dfrac{p_1 + p_2}{2}$ $\vec{u} \approx -\dfrac{1}{\rho \Delta r} \int (\Delta p)\, dt$
  - Intensity: $\vec{C} = E\left[p(t)\vec{u}^*(t)\right]$ ⇒ $\hat{\vec{C}} = -\dfrac{1}{2\rho\Delta r} E\left\{\left[p_1(t) + p_2(t)\right] \int \left[p^*_2(t) - p^*_1(t)\right] dt\right\}$
  - Active intensity: $\hat{\vec{I}} = \mathrm{Re}\left[\hat{\vec{C}}\right] = \dfrac{2}{\omega\rho\Delta r} \mathrm{Im}\left[S_{P_1 P_2}(\omega)\right] = -\dfrac{\mathrm{Im}\, G_{12}}{\omega\rho\Delta r}$

- **Implementation** (sweep or point-wise averaging)
  - FFT (indirect) method or digital filter (direct) method

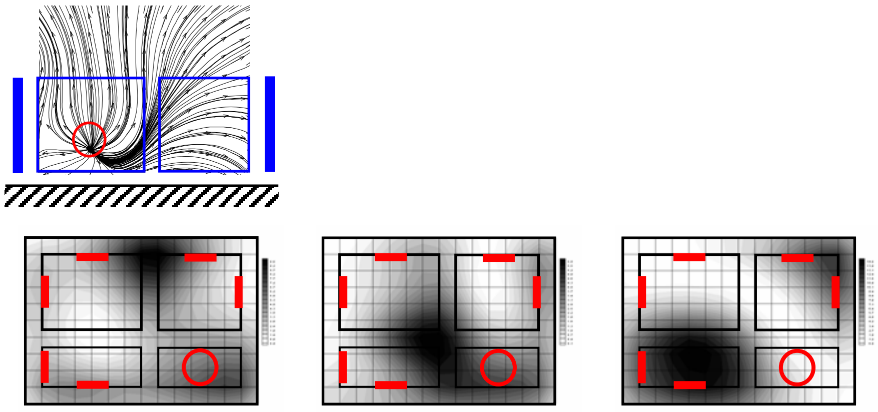

- Near-field vortex of intensity
- Sensitive to field reactivity
- Ease in implementation

Inverse Spherical Expansion of Sound Field

❖ Expansion with single-point, multipoles (e.g., HELS)

- **Approximated solution with *J* spherical radiation functions**

$$p_f(\mathbf{r}_m,\omega)=\sum_{n=0}^{N}\sum_{l=-n}^{n}C_{n,l}h_n(kr_m)Y_n^l(\theta,\phi)=\sum_{j=1}^{J}C_j\psi_j(\mathbf{r}_m,\omega)$$

spherical function

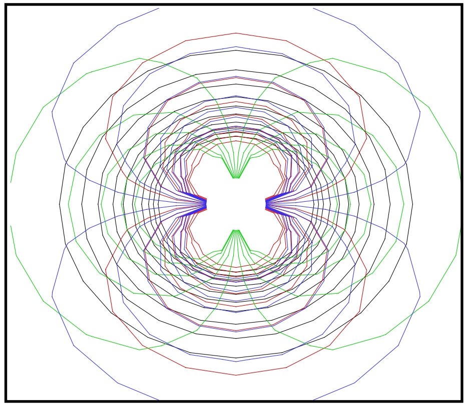

- **Matrix form for *M* measurements**

$$\begin{bmatrix} p_f(\mathbf{r}_1,\omega) \\ p_f(\mathbf{r}_2,\omega) \\ \vdots \\ p_f(\mathbf{r}_M,\omega) \end{bmatrix}_{M\times 1} = \begin{bmatrix} \psi_1(\mathbf{r}_1,\omega) & \psi_2(\mathbf{r}_1,\omega) & \cdots & \psi_J(\mathbf{r}_1,\omega) \\ \psi_1(\mathbf{r}_2,\omega) & \psi_2(\mathbf{r}_2,\omega) & \cdots & \psi_J(\mathbf{r}_2,\omega) \\ \vdots & \vdots & \ddots & \vdots \\ \psi_1(\mathbf{r}_M,\omega) & \psi_2(\mathbf{r}_M,\omega) & \cdots & \psi_J(\mathbf{r}_M,\omega) \end{bmatrix}_{M\times J} \begin{bmatrix} C_1(\omega) \\ C_2(\omega) \\ \vdots \\ C_J(\omega) \end{bmatrix}_{J\times 1}$$

System equation

$$\mathbf{C}=\mathbf{\Psi}^{+}\mathbf{p}_f$$

- Optimal no. of expansion terms
- Optimal selection of field pts
- Fits well to spherical sources only

Spatial-*FT* Based, '*Regular*' Acoust. Holography

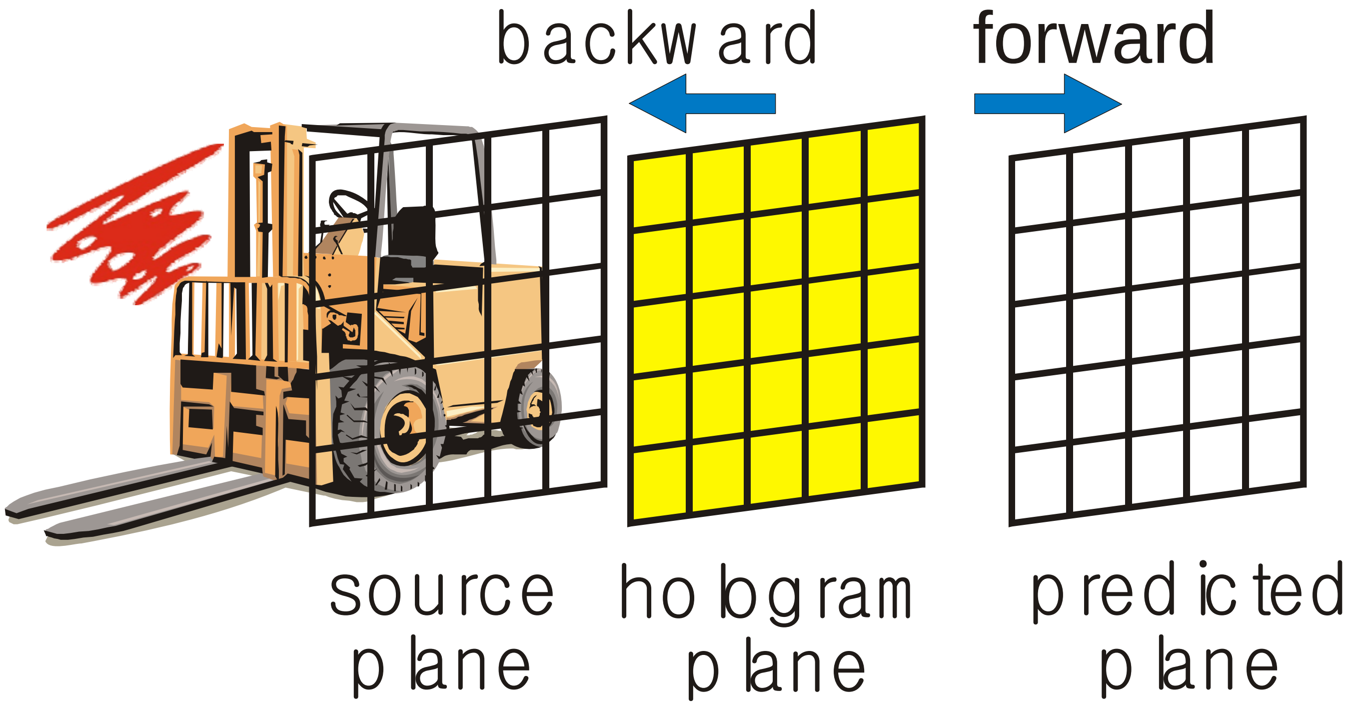

$$p_s = \mathbf{F}^{-1}[e^{+j\,k_z\,(z_h - z_s)}\mathbf{F}[p_h]]$$

- Separable coordinates only
- Leakage
- Hypothetical regular plane for complex-shaped source

N.B. *"Source" plane is not the "true source" plane for inseparable coordinates*

BEM-based, ‘*Non-regular*’ Acoust. Holography

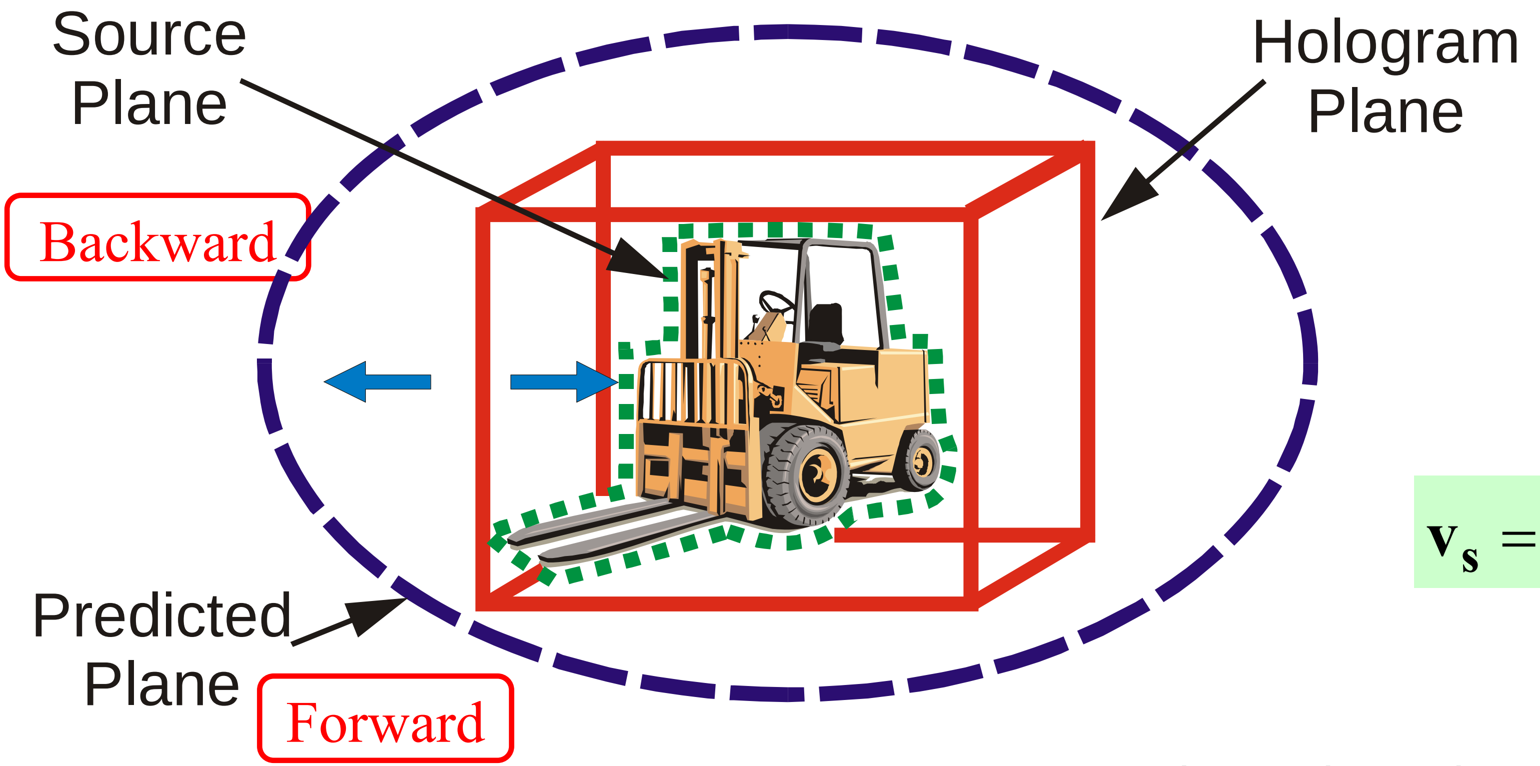

$$\mathbf{v}_s = \mathbf{G}^+ \mathbf{p}_f$$

- Singularity prob.: regularization
- Additional BEM modeling
- Freq. limitation due to BE size
- Ease in forward calc. (BEM)

N.B. *Reconstructed “source” plane coincides with “true source” plane.*

Inverse FRF, Holographic Method

▪ **Construction of system FRF matrix**

► **Calibration process**

$$P(\omega)_m = H(\omega)_{m\times n} Q(\omega)_n$$

▪ **Calculation of inverse FRF matrix**

$$\mathrm{H}^{+} = \left(\mathrm{H}^{H}\mathrm{H}\right)^{-1}\mathrm{H}^{H}$$

► **Identification process**

$$\tilde{Q}(\omega)_n = H(\omega)^{+}_{n\times m} \tilde{P}(\omega)_m$$

▪ **Identification of actual noise source**

$$\mathbf{v_S S_S} = \mathbf{H^{+} p_f}$$

Actual noise source
= Linear combination of ideal sources

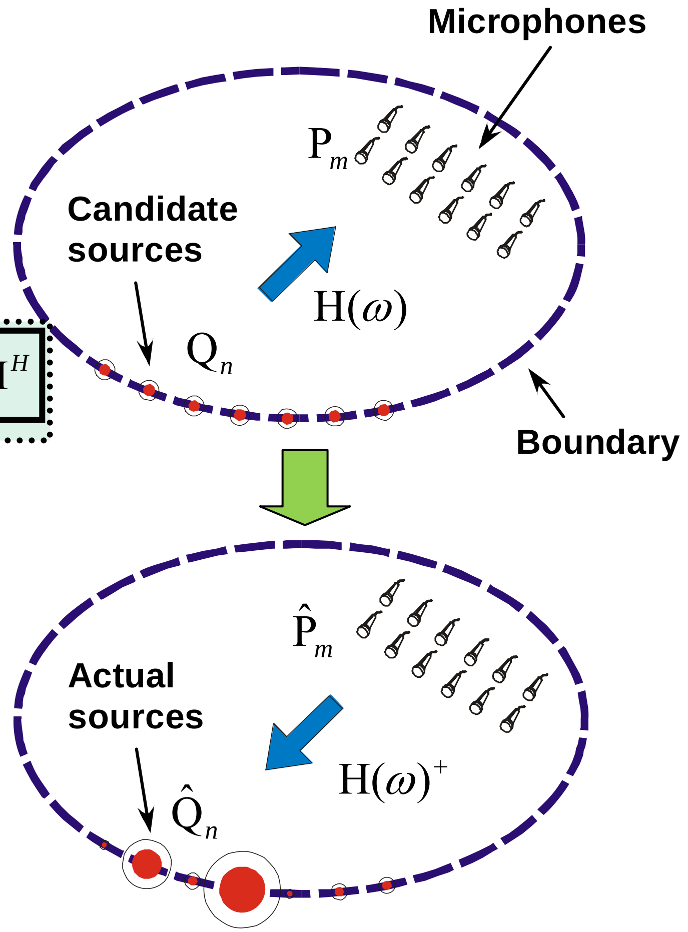

- Singularity prob.: field absorption, regularization
- Coarse spatial resolution
- Prob. in source treatment
- Easy in concept & application